An NMR and Molecular Modeling Study of the Site-Specific Binding of Histamine by Heparin, Chemically Modified Heparin, and Heparin-Derived Oligosaccharides†

Wei-Lien Chuang, Marie Dvorak Christ, Jie Peng, and Dallas L. Rabenstein*

Department of Chemistry, University of California Riverside, California 92521

Received November 10, 1999; Revised Manuscript Received December 28, 1999

ABSTRACT: The diprotonated form of histamine binds site-specifically to heparin, a highly sulfated 1→4 linked repeating copolymer comprised predominantly of 2-O-sulfo-α-L-iduronic acid (the I ring) and 2-deoxy-2-sulfamido-6-O-sulfo-α-D-glucopyranosyl (the A ring). The binding is mediated by electrostatic interactions. The structural features of histamine and heparin, which are required for the site-specific binding, have been identified from the results of ^{1}H NMR studies of the binding of histamine by six heparin-derived oligosaccharides and four chemically modified heparins and molecular modeling studies. The results indicate that the imidazolium ring of diprotonated histamine is critical for directing site-specific binding, while the ammonium group increases the binding affinity. The imidazolium ring binds within a cleft, with the A ring of an IAI triad at the top of the cleft, and the I rings forming the two sides. The H3 proton of the A ring is in the shielding cone of the imidazolium ring. The carboxylate group of the I-ring at the reducing end of the IAI triad and possibly the sulfamido group of the A-ring are essential for site-specific binding, whereas the 2-O-sulfate group of the I ring and the 6-O-sulfate group of the A ring are not. The results indicate that histamine binds to the IAI triad with the I rings in the $^1C_4$ conformation. Also, the configuration of the carboxylate group is critical, as indicated by the absence of site-specific binding of histamine by the related IAG sequence, where G is α-D-glucuronic acid. The molecular modeling results indicate that the N1H and N3H protons of the imidazolium ring of site-specifically bound histamine are hydrogen bonded to the carboxylates of the I rings at the nonreducing and reducing ends of the IAI trisaccharide sequence.

Tissue histamine is stored in the membrane-enclosed secretory granules of mast cells (*1*, *2*). The results of ^{1}H NMR experiments on intact mast cells and isolated mast cell granules indicate that the histamine in mast cells must be relatively mobile and not rigidly associated with the granule matrix (*3*). Resonances were not observed for the granule matrix and thus no information could be obtained about the nature of the storage mechanism (*3*); however, evidence suggests that the histamine binds to the heparin of the granule matrix (*4*−*7*).

Heparin is a highly negatively charged, 1→4 linked copolymer of either iduronic or glucuronic acid and D-glucosamine. The structure of heparin is largely accounted for by repeating sequences of the trisulfated disaccharide [→4)-IdoA(2S)−(1→4)-GlcNS(6S)−(1→] where IdoA(2S) and GlcNS(6S) represent 2-O-sulfo-α-L-iduronic acid and 2-deoxy-2-sulfamido-6-O-sulfo-α-D-glucopyranose, the I-ring and A-ring, respectively, in the following structure.[1]

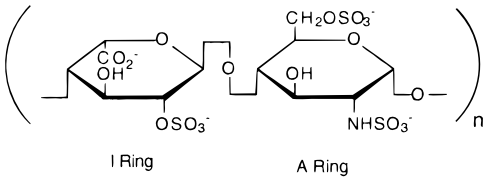

For example, this repeating disaccharide accounts for at least 85% of heparins from beef lung and about 75% of those from porcine intestinal mucosa (*8*, *9*). Minor constituents,

† Research supported in part by the National Institutes of Health Grant HL56588 and by the University of California, Riverside, Committee on Research. Funding for the Varian Unity Inova 500 spectrometer was provided in part by NSF-ARI Grant 9601831.

* To whom correspondence and reprint requests should be addressed. Telephone: (909)787-3585. Fax: (909)787-2435. E-mail: dallas.rabenstein@ucr.edu.

[1] Abbreviations: IdoA(2S), 2-O-sulfo-α-L-iduronic acid; GlcNS(6S), 2-deoxy-2-sulfamido-6-O-sulfo-α-D-glucopyranose; GlcA, D-glucuronic acid; GlcNAc, *N*-acetyl-glucosamine; ΔU(2S), 4,5-unsaturated-2-O-sulfo-uronic acid; NMR, nuclear magnetic resonance; TOCSY, total correlation spectroscopy; ROESY, rotating frame Overhauser enhancement spectroscopy. Residue abbreviations are used in defining an oligosaccharide chain and a specific proton in the chain. For example, ΔUA(2S)-(1→4)-GlcNS(6S)-(1→4)-IdoA(2S)-(1→4)-GlcNS(6S)-(1→4)-GlcA-(1→4)-GlcNS(6S) is abbreviated ΔUAIAGA where ΔU represents ΔU(2S), A represents GlcNS(6S), I represents IdoA(2S), and G represents GlcA. The sequential position of a residue in an oligosaccharide is identified by an alphanumeric character: a denotes the residue at the nonreducing end and subsequent residues are labeled in alphabetic order in the direction of the reducing end. For example, Ab, Ad, and Af refer to the three A residues in the ΔUAIAGA hexasaccharide. Proton location is specified by residue, sequence position and ring position, e.g., Ab-H3 refers to the proton at ring postion 3 in the Ab residue. A prime (′) denotes the nonreducing end position in a chain sequence; a double prime (″) denotes a reducing end position.

10.1021/bi9926025 CCC: $19.00
Published on Web 03/08/2000

including D-glucuronic acid and 2-deoxy-2-acetamido-6-O-sulfo-α-D-glucopyranose, are present in varying amounts, depending on the source of the heparin. Because of its high negative charge density, heparin is a polyelectrolyte, with a fraction of its negative charge neutralized by bound counterions (*10*−*15*). Counterions can bind to polyelectrolytes by site-specific and by territorial (or delocalized) electrostatic interactions (*16*, *17*).

To determine if histamine binds to heparin, and if the binding is site-specific or territorial, the interaction of histamine with heparin in aqueous solution was studied by ^{1}H and ^{13}C NMR (*6*). It was found that histamine binds to heparin and that, at the pH in mast cell granules (5.2−6.0) (*18*, *19*), the binding is site specific, with the imidazolium group of the diprotonated form of histamine located in a binding pocket, as indicated by an upfield ring-current shift in the resonance frequency for the H3 proton of the A ring (A−H3)[1] (*6*). The binding pocket was found to have a high specificity for imidazolium groups in general, as indicated by the site-specific binding of the imidazolium ion, the imidazolium group of *N*-acetylhistamine and the imidazolium side chain of the tripeptide glycyl-histidyl-lysine in the same binding pocket (*6*, *20*). Histamine-heparin binding is mediated primarily by electrostatic interactions (*7*); however, the features of heparin, which are essential for site-specific binding of histamine, have not been identified.

The interactions involved in the binding of the imidazolium group by heparin are also of interest with regard to the binding of histidine-containing peptides and proteins by heparin, including β-amyloid peptides (*21*) and mouse mast cell protease 7 (mMCP-7) (*22*). The β-amyloid fibrils within the cerebral cortex and hippocampus of the Alzheimer disease brain are associated with heparan sulfate proteoglycan and other macromolecules (*23*). Heparin induces aggregation of β-amyloid peptides, and the pH dependence of the aggregation indicates that the imidazolium side chains of histidines at positions 13 and 14 within the consensus heparin-binding domain (residues 12−17) are involved (*21*). In the case of mMCP-7, the enzyme is stored as a heparin complex in the secretory granules of mast cells, and the binding interaction involves the positively charged side chains of histidines at positions 8, 68, and 70 (*22*).

Because of the importance of the binding of biological molecules by heparin and related glycosaminoglycans (*24*) and the general lack of detailed information about the interactions involved in binding at the molecular level, we have studied the binding of histamine by the heparin-derived oligosaccharides and the chemically modified heparins shown in Figure 1 and by molecular modeling, with the goal of identifying the structural features which are required for the site-specific binding of histamine. Oligosaccharides **I**−**VI** were prepared by heparinase depolymerization of heparin, which introduces a 4,5-unsaturated uronic acid residue at the nonreducing end. Oligosaccharides **I**−**III** are the fully sulfated di-, tetra-, and hexasaccharides; hexasaccharide **IV** has a glucuronic acid at residue e, while the A rings at positions d and f in hexasaccharide **V** lack the 6-O-sulfate group.[1] The iduronic acid residue at position c of pentasaccharide **VI** lacks the 2-O-sulfate group and there is a glucuronic acid residue at position e. The 2-O-sulfate group of the iduronic acid residue and the 6-O-sulfate group and N-sulfate groups of the glucosamine residue have been removed in various combinations in the four chemically modified heparins (**VIII**−**XI**), and in **XI**, the ammonium group of the glucosamine residue has been acetylated. The results of the experimental and molecular modeling studies taken together indicate the structural features of heparin which are essential for site-specific binding of histamine.

EXPERIMENTAL SECTION

Materials. Bovine lung heparin, porcine intestinal mucosal heparin, *N*-acetyl-de-O-sulfated heparin, histamine and flavobacterium heparinase I (EC 4.2.2.7) were obtained from Sigma Chemical Co.

Heparin-derived Oligosaccharides. The heparin-derived oligosaccharides were prepared using enzymatic digestion and chromatographic purification methods that have been described in detail elsewhere[2] (*25*, *26*). Briefly, 1 g of bovine lung heparin was dissolved with 250 units of heparinase I in 50 mL of digestion buffer (0.1 M sodium acetate, 30 mM calcium acetate, and 0.02% sodium azide) and the solution incubated at 30 °C for 24 h. The solution was concentrated by lyophilization and the resulting material purified using gel permeation chromatography to separate the heparin fragments into fractions of homogeneous size. The sized fractions were collected, desalted, and then, subjected to strong anion exchange (SAX) chromatography to separate the heterogeneous mixtures into pure oligosaccharides. The SAX chromatography was accomplished with a semipreparative CarboPac PA1 HPLC column connected to a Dionex 500 ion chromatography system equipped with an AD20 UV−vis detector. Oligosaccharides were eluted with a linear NaCl gradient (0−2 M NaCl) in phosphate buffer at pH 3. Oligosaccharides **I** and **II** in Figure 1 were obtained from the disaccharide and tetrasaccharide fractions, while hexasaccharides **III** and **IV** were obtained from the hexasaccharide fraction.

The same general procedure outlined above was applied to porcine intestinal mucosal heparin, with the modification that histamine was added to the enzyme digest in order to alter the heparin cleavage pattern of the heparinase I enzyme.[2] A histamine/heparin disaccharide molar ratio of 4:1 produced the largest change in heparin hexasaccharide product distribution compared to the digest without histamine and was thus used in this work. Twelve purified oligosaccharides were recovered from the hexasaccharide fraction, two of which (**V** and **VI** in Figure 1) were used in this study. Although **VI** is a pentasaccharide, it eluted from the gel permeation chromatography column in the hexasaccharide fraction.[3] HPLC-purified oligosaccharides **I**−**VI** were all of greater than 90% purity, as determined by integration of resonances in the anomeric region of their 1D ^{1}H NMR spectra.

Heparin Polysaccharide Desulfation. 2-O-desulfated heparin, **VIII** in Figure 1, was produced by alkaline desulfation as described by Jaseja et al. (*27*). Bovine heparin (sodium salt) was dissolved in water adjusted to pH 12.5 with sodium

[2] Chuang, W.-L., McAllister, H., and Rabenstein, D. L., unpublished results.

[3] Oligosaccharide VI is unusual as a product of the heparinase-catalyzed depolymerization of heparin in that it contains an odd number of sugar rings and is terminated at the reducing end by glucuronic acid. This pentasaccharide, which has been reported previously, appears to be derived from the reducing end of a parent heparin chain (*43*).

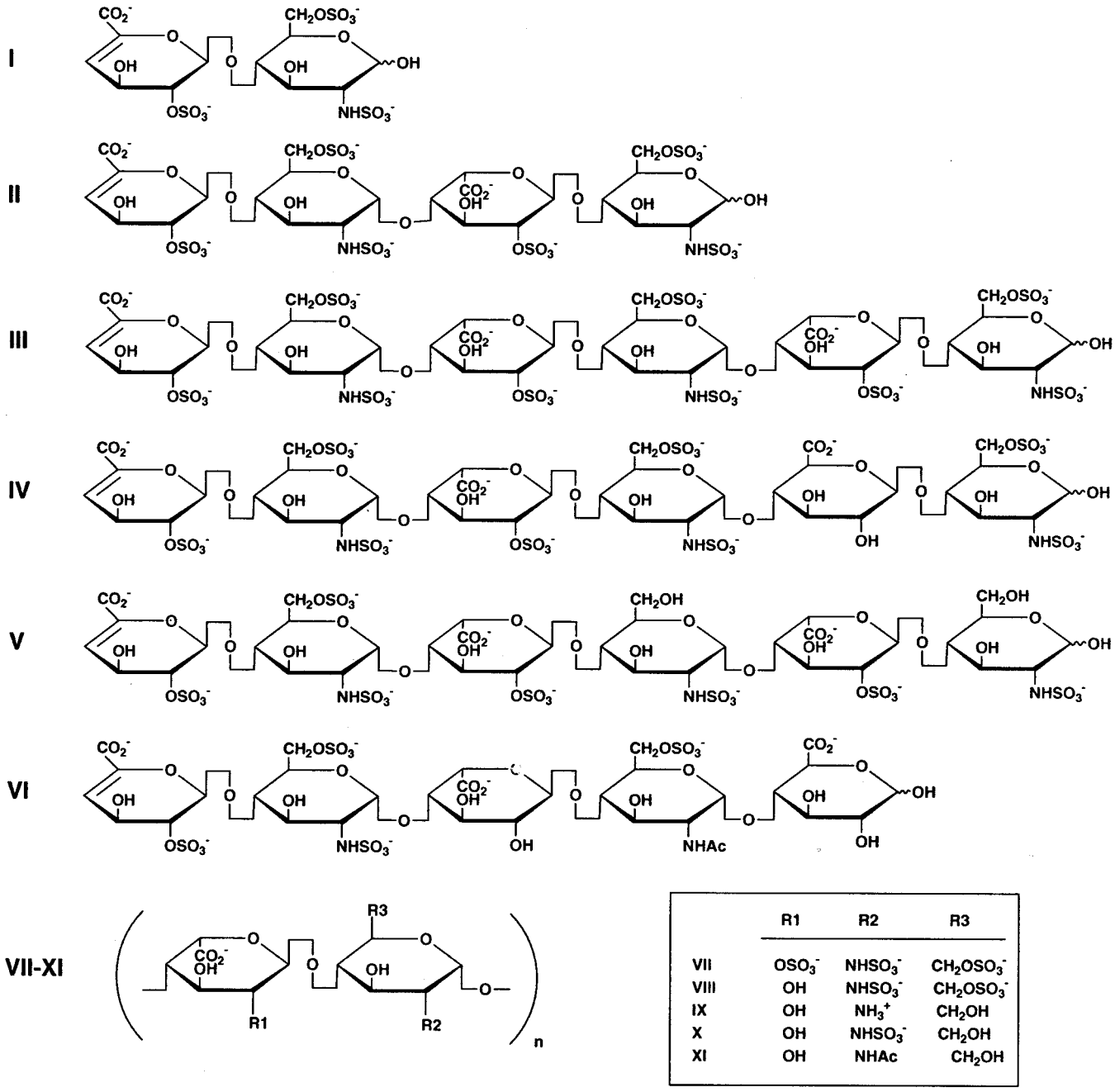

FIGURE 1: Heparin-derived oligosaccharides and chemically modified heparin polysaccharides.

hydroxide. The solution was lyophilized to dryness and desalted on a Sephadex G15 column. 2-O-desulfation was 88% complete, based on integration of the anomeric region of the 1D ^{1}H NMR spectrum.

Fully desulfated heparin, **IX**, was prepared by solvolytic desulfation, using conditions specified by Nagasawa and Inoue (*28*). Specifically, 200 mg of dry bovine heparin (pyridinium salt) were dissolved in a solution of DMSO containing 10% methanol and heated for 24 h at 105 °C. To isolate product, the solution pH was adjusted to 9.0, the polysaccharide was precipitated with 10 volumes of cold ethanol saturated with sodium acetate, and the precipitate was recovered by centrifugation. To remove residual DMSO and to convert the product to its sodium salt, the precipitate was dissolved in 0.1 M NaCl and desalted on a Sephadex G15 column.

N-sulfated-O-desulfated heparin, **X**, was produced by selective N-sulfation of unsulfated heparin, **IX**, using established methods (*29*). Unsulfated heparin (sodium salt) was dissolved in Millipore water adjusted to pH 9.0 with saturated sodium carbonate solution. Trimethylamine sulfur trioxide complex was added to the solution, which was then heated at 55 °C. After 3 h, a second aliquot of trimethylamine sulfur trioxide was added, and the solution was heated for an additional 3 h. The heparin product was isolated by ethanol precipitation as described above.

NMR Sample Preparation. Oligosaccharide solutions of 1−5 mM were prepared in 99.98% D_2O. Aliquots of concentrated histamine solution (0.5 M) were added to achieve molar ratios of histamine/heparin oligosaccharide ranging from 0 to 10. Solutions were lyophilized and then redissolved in D_2O. This cycle was repeated several times

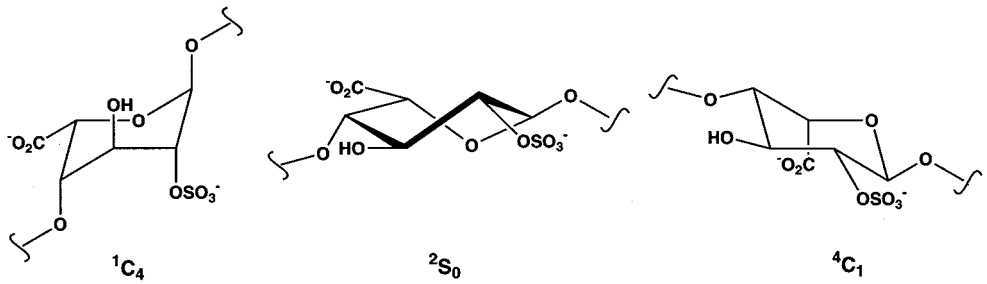

FIGURE 2: The $^1C_4$, $^2S_0$, and $^4C_1$ conformers of 2-O-sulfo-α-L-iduronic acid.

to reduce the intensity of the residual HDO resonance. Samples also contained sodium 3-(trimethylsilyl) propionate-2,2,3,3-d_4, which was added as a chemical shift reference, and 10 ppm EDTA-d_{12}, which was added to reduce line broadening caused by paramagnetic cations. Solution pD was adjusted directly in the NMR tube and was monitored with an Ingold combination ultramicroelectrode. Shigemi NMR tubes were used to reduce sample volumes (~320 μL) and to improve suppression of the HDO resonance. A similar procedure was used with the chemically modified heparins; concentrations of 1−5 mM were used where the concentration is expressed in terms of the concentration of the disaccharide repeat unit.

NMR Spectroscopy. ^{1}H NMR spectra were measured at 500 MHz on a Varian Unity Inova spectrometer equipped with waveform generators, a Performa X,Y, Z gradient module and a ^{1}H{^{13}C,^{15}N} triple resonance X,Y, Z triple axis pulsed field gradient probe. Spectra were measured at temperatures in the range of 5−35 °C and the HDO resonance was suppressed using a selective saturation pulse during the relaxation delay. 2D-TOCSY and 2D-ROESY spectra (*30*−*33*) were measured in the phase-sensitive mode by the hypercomplex method of States et al. (*34*).

^3J-coupling constants were determined from spectra measured using a 1D-TOCSY pulse sequence (*35*). A shaped Gaussian pulse (60−75 ms) was used for selective inversion. A z-filter was applied utilizing an array of delays in the range of 1−20 ms, calculated as prescribed by Rance (*36*). An MLEV17 spin lock (*30*) of approximately 4.5 kHz field strength was applied for 170 ms. Chemical shifts and ^3J-coupling constants were extracted by simulation of 1D spectra using Varian's implementation of the LAOCOON spin simulation program (*37*).

Conformational averaging of theoretical coupling constants was used to extract the populations of the $^1C_4$, $^2S_0$ and $^4C_1$ iduronate conformers (Figure 2) from experimentally determined coupling constants (*38*). The following set of linear equations was solved using least-squares minimization:

$$J^{\exp}_{i,i+1} = P^1{}_{C_4} J^{^1C_4}_{i,i+1} + P^2{}_{S_0} J^{^2S_0}_{i,i+1} \quad (1)$$

where $J^{\exp}_{i,i+1}$ is the experimental three-bond coupling constant of the vicinally related i and i+1 ring protons (i = 1−5), and $J^{^1C_4}_{i,i+1}$ and $J^{^2S_0}_{i,i+1}$ are theoretical values of the coupling constants and $P^1{}_{C_4}$ and $P^2{}_{S_0}$ the normalized populations of the indicated conformations.

Computational Methods. Molecular modeling was used to investigate the specific sites of interaction between histamine and heparin. Modeling calculations were performed with Insight II and Discover95 software packages from Molecular Simulations, Inc., running on a Silicon Graphics Indigo 2 workstation. The Amber force field (Discover Version 2.4), which includes Homan's carbohydrate-specific parameters (*39*), was employed in all energy calculations. A distance-dependent dielectric was utilized in all calculations with ϵ = 4 and a 0.5 scale factor was used for the 1−4 nonbonded interactions. All bond parameters were explicitly defined requiring addition of parameters for ester sulfate and sulfamido substituents as prescribed by Huige and Altona (*40*). The partial charges on the ester sulfate and sulfamido groups were assigned to closely match the ab initio calculated charges of methyl sulfate and methyl sulfamate reported in their study. Parameters for the imidazolium ring of histamine were adapted from standard Amber parameters for histidine in its cationic imidazolium state.

Heparin oligosaccharides were built from I and A residue structures derived from X-ray coordinates. Cartesian coordinates for the I ring in the $^1C_4$ conformation and the A ring in the $^4C_1$ conformation were obtained from the Brookhaven Protein Data Bank X-ray structure of the heparin tetrasaccharide ΔUAIA[1] bound to fibroblast growth factor (*41*). Coordinates for the I ring in the $^2S_0$ conformation were obtained from the X-ray structure of methyl 4,6-O−(S)-benzylidene-2-chloro-2-deoxy-α-D-idopyranoside (*42*).

Energy maps were calculated for the A(1→4)I and I(1→4)A glycosidic bonds as a function of ϕ and ψ torsion angles, as defined by the following I(1→4)A disaccharide segment of heparin.

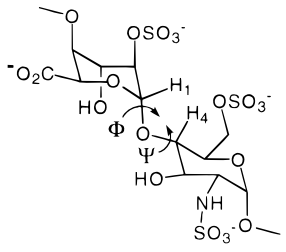

Φ is the dihedral angle defined by H1-C1-O-C4″ and ψ the dihedral defined by C1−O−C4"-H4" where the double primes denote atoms of the residue at the reducing end of the oligosaccharide.[1] Residues were linked into AI and IA disaccharides using a glycosidic angle of 117°. One pair of AI and IA disaccharides was constructed with the I rings in the $^1C_4$ conformation and a second pair with the $^2S_0$ conformation. Rigid energy maps were calculated for each of the four disaccharide structures using the dihedral driver routine provided with Discover. Φ and Ψ dihedral angles were incremented in 20° intervals, while all other internal coordinates were fixed. Φ and Ψ loci corresponding to the energy minima were identified and used to construct a set

Table 1: Heparin Trisaccharide Structures Docked to Histamine

			I ring conformation[a]		grid search 10 Kcal domain range			
trisaccharide	$(\phi/\psi)_{IA}$	$(\phi/\psi)_{AI}$	I′	I″	ϕ_{IA}	ψ_{IA}	ϕ_{AI}	ψ_{AI}
1	40/−20	−20/−20	$^1C_4$	$^1C_4$	0 to 80	20 to −60	−50 to 60	−30 to 40
2	−60/−60	−20/−20	$^1C_4$	$^1C_4$	0 to −70	−80 to −40	−50 to 60	−30 to 40
3	60/0	−50/−40	$^2S_0$	$^2S_0$	−20 to 80	−60 to 40	−80 to 0	−80 to 0

[a] A prime denotes the nonreducing end I ring, a double prime denotes the reducing end I ring.[1]

of candidate heparin trisaccharide structures for histamine docking calculations. Each of the candidate heparin trisaccharide structures defined in Table 1 was a function of two independent pairs of Φ/Ψ dihedral angles and the I ring conformation.

Histamine−Heparin Trisaccharide Complexes. The following procedure was used to identify the most energetically favorable orientation of histamine and heparin in the bound complex. Three IAI trisaccharides were constructed using the I and A monomer structures described above and glycosidic dihedral angles, which were selected from the low energy regions of the disaccharide energy maps. Each trisaccharide was fully minimized, allowing relaxation of all internal coordinates, with simultaneous application of a forcing potential to maintain the glycosidic torsion angles defining each trisaccharide.

Docking of histamine to each trisaccharide was evaluated in order to identify the most energetically favorable complex. Histamine was manually docked to each heparin trisaccharide, while monitoring the intermolecular energy in real time using the Discover software Docking Module. Histamine was located adjacent to the A residue in an orientation which positioned A−H3[1] within the shielding cone of the imidazole ring. Further manual refinement of the histamine position was employed to prevent any highly energetic steric collisions of the two molecules. Manual docking produced six different histamine−trisaccharide complexes, which were subjected to a grid search calculation.

Grid search describes a systematic search algorithm used to identify the lowest energy complex in the region of conformational space surrounding the manually docked complex. The ϕ_{IA}, ψ_{IA}, Φ_{AI}, and ψ_{AI} torsion angles of the trisaccharide in the complex were successively incremented to generate the four-dimensional grid of structures included in the search.

The bounds of the grid search reported in Table 1 were defined approximately by the 10 kcal region surrounding each of the minima located in the energy maps of Figure 3. Each of the docked structures in the grid was minimized using a procedure where the partial charges were progressively turned on. Partial charges were initially scaled to 0.5 for 200 iterations, then scaled to 0.7 for 200 iterations, and finally scaled to 1.0 for 400 iterations. Imidazole distance constraints were imposed during the minimization to ensure that the A−H3 proton remained within the shielding cone of the imidazole ring. The distance from A−H3 to each of the carbon and nitrogen atoms of the imidazole ring was constrained to a range of 2.5−3.5 Å. This positions the plane of the ring so that a perpendicular drawn from the ring's center would roughly intersect the A−H3 proton.

Following minimization of one complex, the next complex in the set was automatically generated by imposing a forcing potential of 100 kcal/mol to rotate one of the ϕ/ψ angles by 20°. This procedure resulted in a relatively smooth transition from one complex to the next in spanning the grid of candidate structures.

RESULTS

The site-specific binding of histamine by heparin was studied by ^{1}H NMR and molecular modeling. In the NMR studies, binding at specific sites in the heparin-derived oligosaccharides was monitored by measuring chemical shift vs pD titration curves for each proton of the oligosaccharide, both free in solution and in solution with histamine. The studies will be illustrated with experimental results for hexasaccharide **III**.

Assignment of ^{1}H NMR Spectra. The one-dimensional ^{1}H NMR spectrum of hexasaccharide **III** in solution with histamine is shown in Figure 4. The triplets at 3.172 and 3.361 ppm and the singlets at 7.406 and 8.629 are from histamine and the resonance at 4.91 ppm is from HDO. The remainder of the resonances are from **III**. Of the thirty-five multiplets that comprise the spectrum of **III**, those for the anomeric protons (5.2−5.5 ppm) are the most resolved. The first step in the asignment procedure was to determine the type of monosaccharide giving each anomeric resonance using subspectra obtained from the TOCSY spectrum. A portion of the TOCSY spectrum is shown in Figure 5, together with subspectra obtained by taking traces through the TOCSY spectrum at the chemical shifts of the anomeric protons. From the patterns of resonances in the subspectra, the resonances at 5.20, 5.31, and 5.45 ppm were assigned to the anomeric protons of iduronic acid residues and those at 5.325, 5.385, and 5.43 ppm to the anomeric protons of glucosamine residues. The resonances in each subspectrum were then assigned to specific ring protons with the aid of an extensive database of heparin oligosaccharide ^{1}H chemical shift assignments found in the literature (*43*−*47*). The anomeric resonance at 5.45 ppm was assigned to the ΔUa-H1 proton[1] on the basis of its TOCSY connectivity to the ΔUa-H4 resonance at 5.96 ppm. With this assignment, the resonances at 5.43, 5.385, 5.325, 5.31, and 5.20 ppm were then assigned to Af-H1, Ab-H1, Ad-H1, Ie-H1, and Ic-H1, respectively, using ROESY cross-peaks between H1 and H4 protons on monosaccharide residues linked by a glycosidic bond; the H1−H4 region of the ROESY spectrum is shown in Figure 6, together with the assigned dipolar connectivities.

Chemical Shift vs pH Titration Curves for III. The chemical shift of each proton in **III** was measured as a function of pD over the pD range 2−12, both free in solution and in solution with histamine. Exchange-averaged resonances were observed for both histamine and **III**, indicating fast exchange of both between their free and bound forms on the NMR time scale. Because of extensive overlap in the 1D ^{1}H NMR spectrum, the chemical shift data were obtained

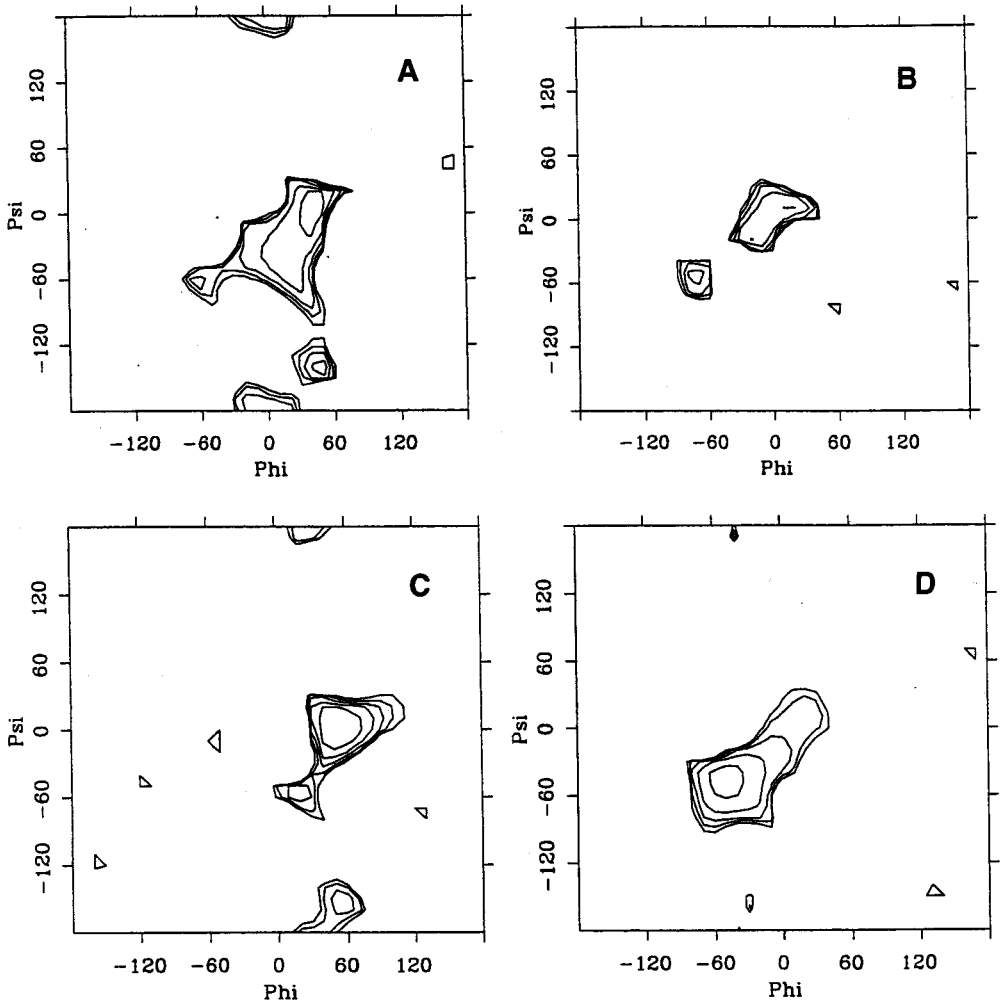

FIGURE 3: Rigid energy maps of heparin glycosidic linkages. (A) I(1→4)A with I in the $^1C_4$ conformation; (B) A(1→4)I with I in the $^1C_4$ conformation; (C) I(1→4)A with I in the $^2S_0$ conformation and (D) A(1→4)I with I in the $^2S_0$ conformation. The global minima for A, B, C, and D are at ϕ,ψ of 40, −20; −20, −20; 60, 0, and -50, −40 degrees, respectively. Contours are separated by 2 kcal/mol intervals.

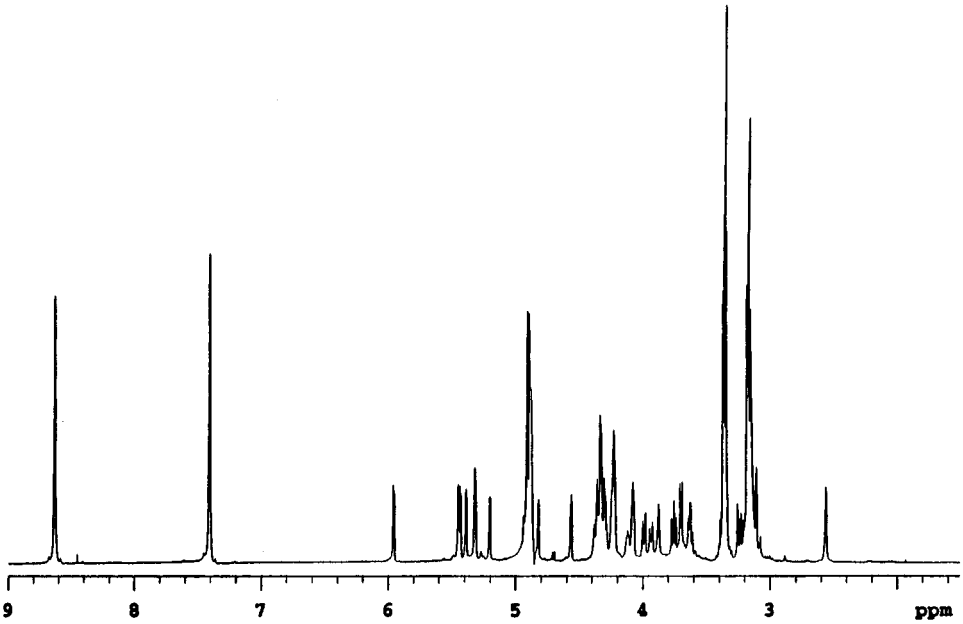

FIGURE 4: 500 MHz ^{1}H NMR spectrum of 4.9 mM hexasaccharide **III** in D_2O solution with 15.1 mM histamine at pD = 6.05 and 10 °C.

from traces taken through the anomeric resonances in 2D-TOCSY spectra (Figure 5), which were measured as a function of pD. The heparin resonances which shift the most in the presence of histamine are H5 of the I ring and H3 of the A ring, with the shift of the H3 resonance of the A ring providing evidence of site-specific binding of histamine (*6*).

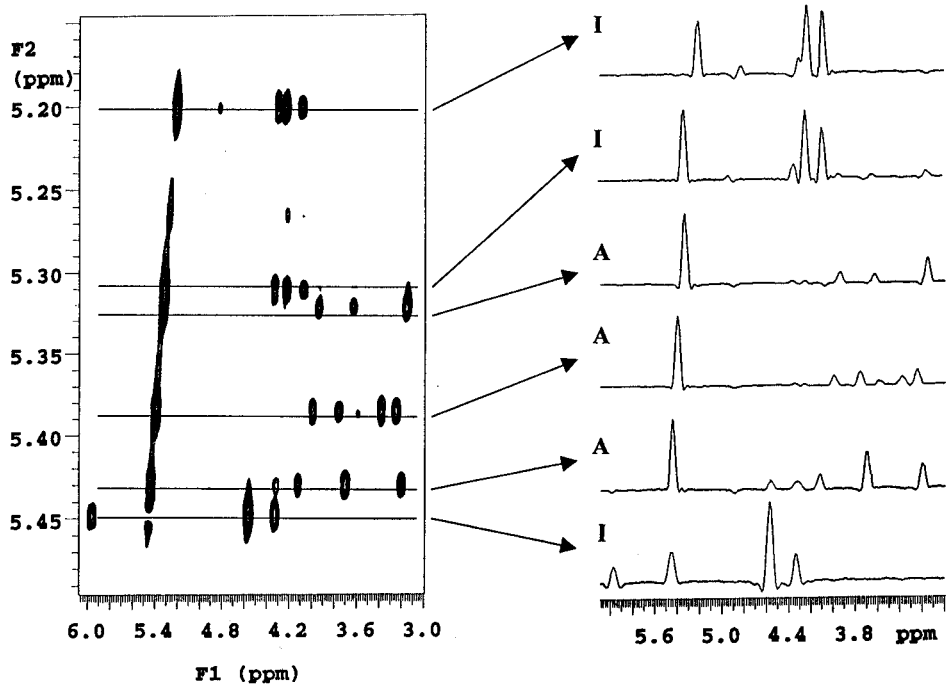

FIGURE 5: A portion of the TOCSY spectrum of the hexasaccharide **III**/histamine solution in Figure 3 and subspectra obtained by taking traces through the TOCSY spectrum as indicated. This region of the TOCSY spectrum was used rather than the F1 = 5.15−5.50 ppm and F2 = 3.0−6.0 ppm region because, with the better resolution in the F2 dimension, the subspectra obtained for each of the six monosaccharide residues are relatively free of resonances from the other monosaccharides; 8 K data points were collected at 128 *t*1 increments, using a mixing time of 120 ms.

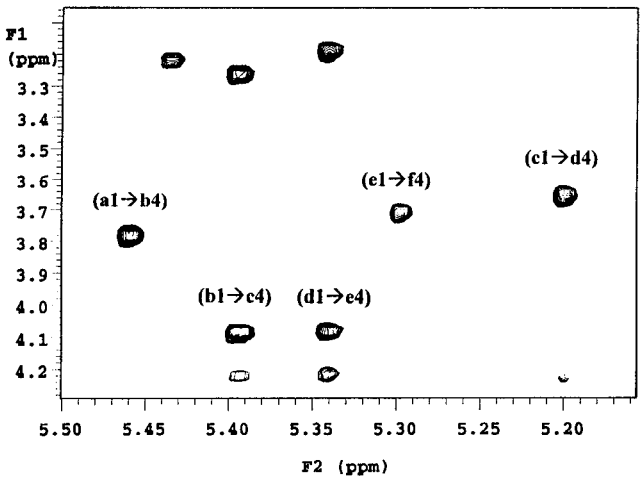

FIGURE 6: A portion of the ROESY spectrum of the hexasaccharide **III**/histamine solution in Figure 3. The dipolar cross-peaks, which establish the sequence of the monosaccharide residues, are identified; 8 K data points were collected at 256 t1 increments, using a mixing time of 200 ms.

Chemical shift data for ΔUa-H4, Ic-H5, and Ie-H5 and for the three A−H3 protons of **III**, both free in solution and in solution with histamine, are presented in Figures 7 and 8, respectively.

The upfield shift of resonances for the ΔUa-H4, Ic-H5, and Ie-H5 protons over the pD range of 2.5−6 reflects titration of the carboxylic acid groups on the ΔUa, Ic, and Ie rings, respectively. pK_A values of 4.03, 4.69, and 4.66 were calculated for the ΔUa, Ic, and Ie carboxylic acid groups using the chemical shift data. In the presence of histamine, the chemical shift vs pD titration curves for ΔUa-H4 and Ic-H5 are displaced to lower pD, consistent with histamine binding to the carboxylate groups of ΔUa and Ic, as described by the following equilibria (*6*):

$$HepCO_2H \rightleftharpoons HepCO_2^- + H^+ \quad (2)$$

$$HepCO_2^- + H_2A^{2+} \rightleftharpoons HepCO_2^- - H_2A^{2+} \quad (3)$$

where $HepCO_2^-$ represents the carboxylate groups of ΔUa and Ic and H_2A^{2+} the diprotonated form of histamine. The chemical shift vs pD titration data for Ie-H5 in the presence of histamine shows a different behavior, which is discussed in a following section.

The resonance for the C2H proton of free histamine shifts over the pD range of 5−8 due to titration of the imidazolium group (data not shown). In the presence of **III**, the chemical shift vs pD titration curve for C2H of histamine is displaced to higher pD by about 1 pD unit, due to formation of the $HepCO_2^- - H_2A^{2+}$ complex.

The chemical shifts of the Ab-H3, Ad-H3 and Af-H3 resonances for **III** are essentially independent of pD in the absence of histamine (Figure 8). However, in the presence of histamine, the resonances for Ab-H3, and Ad-H3 shift upfield over the pD region where the chemical shift data for ΔUa-H4 and Ic-H5 (Figure 7) indicates formation of the $HepCO_2^- - H_2A^{2+}$ complex. The upfield shift reaches a maximum at pD ∼ 6. As the pD is increased further and the $HepCO_2^- - H_2A^{2+}$ complex dissociates, as indicated by the chemical shift vs pD titration data for C2H of histamine, the chemical shifts of the Ab-H3 and Ad-H3 protons move back toward their values in the absence of histamine. The maximum chemical shift, Δδ, defined as the chemical shift of a specific proton of **III** free in solution minus its chemical shift in the histamine/**III** mixture, is reported in Table 2 for

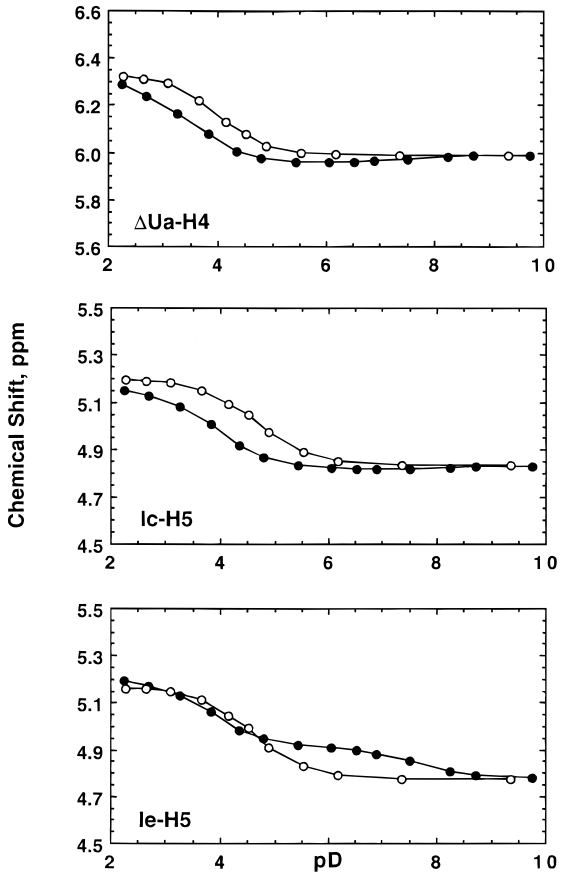

FIGURE 7: Chemical shifts of resonances for the ΔU-H4, Ic-H5, and Ie-H5 protons of hexasaccharide **III** as a function of pD for a solution containing 4.88 mM **III** (open circles) and a solution containing 4.9 mM **III** plus 15.1 mM histamine (filled circles). Measurements were made at 10 °C and the residual HDO resonance was suppressed by presaturation.

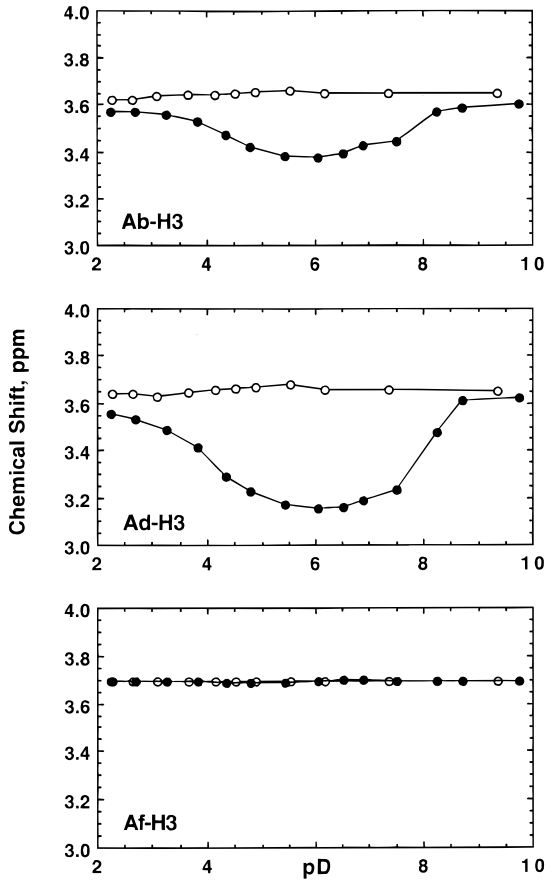

FIGURE 8: Chemical shifts of resonances for the Ab-H3, Ad-H3, and Af-H3 protons of hexasaccharide **III** as a function of pD for a solution containing 4.88 mM **III** (open circles) and a solution containing 4.9 mM **III** plus 15.1 mM histamine (filled circles). Measurements were made at 10 °C and the residual HDO resonance was suppressed by presaturation.

the A−H3 protons of **III**. The $\Delta\delta$s for other protons of Ab and Ad of **III** are: Ab-H1 (0.025 ppm), Ab-H2 (0.045 ppm), Ab-H4 (0.083 ppm), Ab-H5 (0.048 ppm), Ad-H1 (0.124 ppm), Ad-H2 (0.127 ppm), Ad-H4 (0.137 ppm), and Ad-H5 (0.087 ppm).

The upfield shift of the resonances for Ab-H3 and Ad-H3 is analogous to the behavior observed for the A−H3 resonance of heparin in solution with histamine and indicates that there are two site-specific binding sites for histamine in **III**—one centered on residue Ab and the other centered on residue Ad. Notably, the Af-H3 resonance of **III** is not affected by the presence of histamine, indicating the absence of site-specific binding of histamine at residue Af.

On the basis of the magnitude of the equilibrium constant for the binding of histamine by heparin (*7*), both the Ab and Ad binding sites of **III** are only partially occupied under these experimental conditions (Table 1). Also, the relative magnitudes of the $\Delta\delta$s for Ab-H3 and Ad-H3, respectively, at pD 6.0 indicate that there is less binding at site Ab than site Ad, most likely due to there being a ΔU residue rather than an I residue at the nonreducing end of residue Ab.

Minimum Binding Sequence. The proximity of the imidazolium ring of site-specifically bound histamine to an A−H3 proton approximately centers the histamine between two I residues. This together with the absence of site-specific binding at the Af residue of **III** suggests that the IAI triad is the minimum sequence for site-specific binding. Also, molecular models show that the 5 Å length of histamine restricts the size of the histamine binding site to no more than the three residues of the IAI triad. To determine if histamine interacts with only one or with both of the flanking I residues, the binding of histamine by the fully sulfated di- and tetrasaccharides (**I** and **II** in Figure 1) was studied. Chemical shift vs pD titration curves were measured for **I** and **II**, both free in solution and in solution with histamine at a 1:1 molar ratio of histamine to disaccharide repeat unit; the chemical shift vs pD titration curves for the A−H3 protons of **I** and **II** are presented in Figure 9. The chemical shift vs pD titration curve for Ab-H3 of **I** is essentially the same in the absence and presence of histamine, indicating that **I** lacks structural elements which are essential for site-specific binding. For **II**, the chemical shift vs pD titration curve for Ab-H3 shows the upfield shift characteristic of site-specific binding at residue Ab, but that for Ad-H3 is essentially the same in the presence and absence of histamine. These results, together with those for **III**, indicate that a uronic acid residue must be linked to the reducing end of an A residue for it to bind histamine site-specifically.

To probe the sensitivity of binding to the configuration of the uronic acid at the reducing end of the IAI sequence, the binding of histamine by hexasaccharide **IV** was studied. As compared to hexasaccharide **III**, the residue at position e differs both in configuration of the carboxylate group and in the absence of a 2-O-sulfate group. The $\Delta\delta$s for Ab-H3,

Table 2: Maximum Upfield Shifts Induced by Histamine in the H3 Resonance of Glucosamine (A Ring) Residues

heparin oligosaccharide or modified heparin polysaccharide	histamine: heparin[a]	pD	maximum $\Delta\delta$, ppm[b]			
			A-H3	Ab-H3	Ad−H3	Af-H3
I	1:1	6.1		0.02		
II	1:1	5.8		0.19	0.02	
III	1:1	5.9		0.26	0.50	0.00
IV	1:1	6.0		0.23	0.01	0.02
V	4:1	5.5		0.21	0.44	0.04
VI	1:1	6.1		0.24	0.01	
VII	1:1	6.1	0.35			
VIII	2:1	6.0	0.20			
IX	1:1	6.1	0.0			
X	2:1	5.9	0.17			
XI	2:1	5.9	0.0			

[a] Histamine:heparin is defined as the number of moles of histamine per mole of disaccharide repeat unit. [b] $\Delta\delta = \delta_{\text{Free in solution}} - \delta_{\text{In solution with histamine}}$.

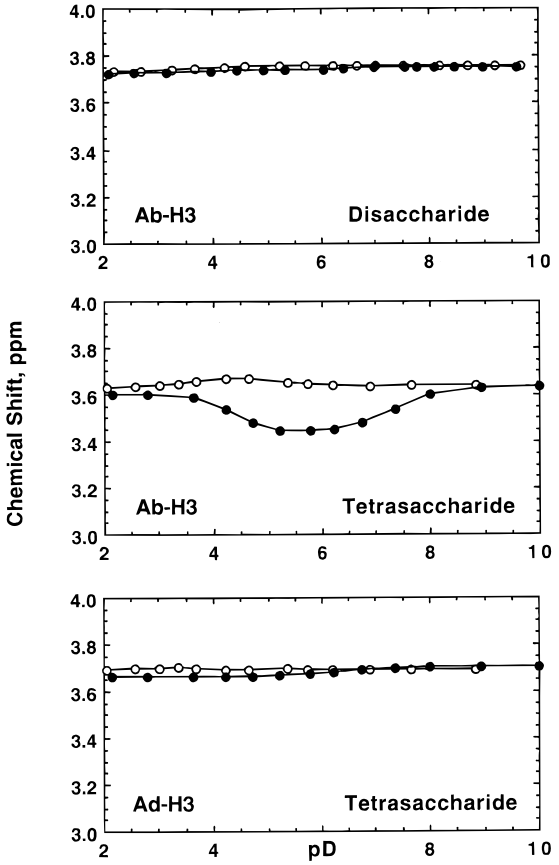

FIGURE 9: (Top frame) Chemical shift of the resonance for the Ab-H3 proton of disaccharide **I** as a function of pD for solutions containing 5.0 mM **I** (open circles) and 5.1 mM **I** plus 4.9 mM histamine (filled circles). (Middle and bottom frames) Chemical shifts of the resonances for the Ab-H3 and Ad-H3 protons of tetrasaccharide **II** as a function of pD for solutions containing 5.0 mM **I** (open circles) and 4.8 mM **II** plus 9.5 mM histamine (filled circles).

Ad-H3, and Af-H3 of **IV** in the presence of histamine at pD 6.5 were 0.23, 0.01, and 0.02 ppm, respectively (Table 2), which indicates site-specific binding at residue Ab, but not at residues Ad and Af. To determine if the lack of site-specific binding to residue Ad is due to the absence of the 2-O-sulfate group on residue e, the binding of histamine by pentasaccharide **VI** in Table 1 and by chemically modified heparin **VIII** was studied. In **VI**, the iduronic acid residue at position c lacks the 2-O-sulfate group, while in **VIII**, the 2-O-sulfate group on the I ring has been selectively removed. Ab-H3 of **VI** is shifted upfield by 0.24 ppm (Table 2) in the presence of histamine, while the A−H3 protons of **VIII** are shifted upfield by 0.20 ppm, indicating site specific binding of histamine by residue Ab of **VI** and by the A residues of **VIII**. Thus, the 2-O-sulfate groups of the I residues of the IAI triad are not essential for site-specific binding of histamine, which indicates that the absence of binding at residue Ad of hexasaccharide **IV** is due to the different spatial orientation of the carboxylate group of the glucuronic acid linked to the reducing end of residue Ad.

The requirements of the I residue at the nonreducing end of the proposed IAI minimum binding sequence could not be definitively resolved. However, the influence of the structure of this residue on the binding strength is evident from results in Table 1. For example, the $\Delta\delta$s for Ab-H3 and Ad-H3 of hexasaccharide **III** indicate approximately half as much binding at the Ab site as at the Ad site, which we attribute to differences in the structures of the ΔU and I residues linked to the nonreducing ends of Ab and Ad.

Effect of Sulfate Substituents on Binding. In the previous section, it was found that the 2-O-sulfate groups of the I residues in the IAI triad are not essential for histamine binding. To probe the sensitivity of binding to the 6-O-sulfate group on the A residue, the binding of histamine by hexasaccharide **V** was studied. The results in Table 2 indicate that histamine binds site-specifically at residue Ad of **V**. Thus, the 6-O-sulfate substituent on A residues is not necessary for site-specific binding of histamine. This is confirmed by results in Table 2, which also indicate site-specific binding of histamine by chemically modified heparin **X** where both the 6-O-sulfate on the A ring and the nonessential 2-O-sulfate on the I ring have been selectively removed.

Two chemically modified heparins (**IX** and **XI** in Figure 1) were used to determine if the N-sulfate substituent is essential for site-specific binding of histamine. The results in Table 2 indicate that histamine is not bound site specifically by **IX** or **XI**. The absence of site-specific binding by **IX** could be due to the cationic charge on its ammonium group rather than removal of the N-sulfate substituent. However, the absence of site-specific binding of histamine by **XI** strongly suggests that the N-sulfate group is essential for site specific binding, although the different steric requirements of the N-acetyl group might also contribute to the

Table 3: Experimental Vicinal Coupling Constants for the I-Rings of Hexasaccharide **III** and Theoretical Values of the Coupling Constants for the I-Ring in the $^1C_4$, $^2S_0$, and $^4C_1$ Conformations[a]

	Ia		Ic		Ie				
	without histamine	with histamine	without histamine	with histamine	without histamine	with histamine	theoretical[b] $^1C_4$	theoretical[b] $^2S_0$	theoretical[b] $^4C_1$
$^3J_{1,2}$	2.89	3.50	2.65	2.34	3.33	2.40	1.82	6.32	7.95
$^3J_{2,3}$	2.50	2.65	5.84	5.20	7.00	4.68	2.57	9.85	9.52
$^3J_{3,4}$	5.01	4.60	3.70	3.50	3.52	3.38	2.58	4.43	9.29
$^3J_{4,5}$			2.83	2.60	2.99	2.52	1.34	2.79	5.15

[a] In units of Hz. [b] Ref *38*.

absence of site-specific binding by **XI**.

Effect of Histamine Binding on Iduronic Acid Ring Conformation. The iduronic acid ring in heparin possesses unusual conformational flexibility compared to most other pyranose sugars (*38*). Typically, the iduronate residues of heparin oligosaccharides and polysaccharides in solution are comprised of an equilibrium mixture of the $^1C_4$ and $^2S_0$ conformers (*38*, *48*−*53*), whereas glucosamine residues exist exclusively in the $^4C_1$ conformation. The $^1C_4$, $^2S_0$, and $^4C_1$ conformers are shown in Figure 2. The 2-O-sulfate group of IdoA(2S) stabilizes the $^1C_4$ conformation, while the presence of carbohydrate substituents at position 4, as for the internal Ic and Ie residues in **III**, hinders the $^4C_1$ conformation (*50*), so that only the $^1C_4$ and $^2S_0$ conformations contribute significantly to the equilibrium for internal iduronate residues (*51*, *53*).

To determine the effect of histamine binding on the conformations of iduronate residues in the IAI triad, the conformational equilibria of Ic and Ie in hexasaccharide **III** were characterized for **III** free in solution and in solution with histamine. The populations of the $^1C_4$ and $^2S_0$ conformations for both Ic and Ie were calculated from experimentally determined $^3J_{i,i+1}$ coupling constants using the theoretical coupling constants reported by Ferro et al. (see Table 3) (*38*), as described in the Experimental Section. $^3J_{i,i+1}$ coupling constants were measured for the Ic and Ie rings of hexasaccharide **III** using the selective 1D-TOCSY experiment to obtain high resolution 1D subspectra. The coupling constants for a pure solution of **III** and for a solution containing a 10:1 molar ratio of histamine to **III** are reported in Table 3. Notably, the experimental $^3J_{i,i+1}$ values for Ic and Ie do not match the theoretical coupling constants for any of the three possible conformers, which indicates significant populations of at least two conformers for both I rings. In particular, $^3J_{2,3}$ values in the range of 5−7 Hz are indicative of a mixture of either $^2S_0$ or $^4C_1$ with $^1C_4$; however, the observation of a small $^3J_{3,4}$ (3.5 Hz) precludes the presence of any significant amount of the $^4C_1$ conformer. Thus, significant populations of both the $^1C_4$ and $^2S_0$ conformers must exist in solutions with and without histamine. This was confirmed in the populations calculated by a least-squares fitting of the experimental data to Equation 1. The results are presented in Table 4. The effect of histamine was to increase the $^1C_4$ conformation by 8% for Ic and 28% for Ie.

Previous studies have shown that the unsaturated uronic acid residue at the nonreducing end of heparin oligosaccharides produced by heparinase depolymerization of heparin exists as an equilibrium mixture of the $^1H_2$ and $^2H_1$ conformations (*54*, *55*). A comparison of the vicinal $^1H-^1H$ coupling constants determined for the ΔUa residue of **III** ($^3J_{1,2} = 2.89$ Hz, $^3J_{2,3} = 2.50$ Hz, and $^3J_{3,4} = 5.01$ Hz without histamine and $^3J_{1,2} = 3.50$ Hz, $^3J_{2,3} = 2.65$ Hz, and $^3J_{3,4} = 4.60$ Hz with histamine) with the theoretical values ($^3J_{1,2} = 2.87$ Hz, $^3J_{2,3} = 2.37$ Hz, and $^3J_{3,4} = 4.67$ Hz for the $^1H_2$ conformation and $^3J_{1,2} = 8.27$ Hz, $^3J_{2,3} = 7.67$ Hz, and $^3J_{3,4} = 2.78$ Hz for the $^2H_1$ conformation) (*54*) indicates that the ΔUa residue of free **III** exists essentially completely in the $^1H_2$ conformation, with a small increase in the population of the $^2H_1$ conformation in the presence of histamine.

Table 4: Populations of the Conformations of the Iduronic Acid Residues of Hexasaccharide **III** Free in Solution and in Solution with Histamine[a]

	Ic Residue		Ie Residue	
conformation	without histamine	with histamine	without histamine	with histamine
$^1C_4$	60	68	45	73
$^2S_0$	40	32	55	27

[a] Populations are reported as percentages.

Binding of Imidazole to Hexasaccharide III. To determine if the ammonium group of histamine is necessary for site-specific binding, the binding of imidazole by hexasaccharide **III** was studied. $\Delta\delta$ values of 0.12 and 0.19 were obtained for Ab-H3 and Ad-H3 from chemical shift vs pD titration curves for pD 6.0 solutions of **III** free in solution and in solution with imidazole at an imidazole:hexasaccharide **III** molar ratio of 4:1, which indicates site specific binding of the imidazolium ion at residues Ab and Ad. Thus, the ammonium group is not necessary for site-specific binding of histamine by heparin.

Molecular Models of the Histamine−Heparin Complex. The rigid energy maps in Figure 2 were calculated for the four disaccharides to establish the ϕ, ψ regions of lowest energy. Energy minima identified in these maps were used in the construction of trisaccharides, as described in the Experimental Section. Three trisaccharides with the IdoA-(2S)-(1→4)-GlcNS(6S)-(1→4)-IdoA(2S) (IAI) sequence but with different glycosidic dihedral angles and I ring conformations, as summarized in Table 5, were constructed for use in the docking experiments.

Histamine was manually docked to each of the trisaccharides. Manual docking facilitated semiquantitative, real-time exploration of the energetics of the conformational space available to the histamine. With all three trisaccharides, histamine was found to fit within a cleft; the A ring forms the top boundary of the cleft with the I′ and I″ residues forming the two sides.[1] Separations of 4 Å between A3 and the imidazole ring were easily obtained, suggesting that smaller separations would be encountered in the refined

Table 5: Calculated Φ, Ψ Angles and Energies for the Various Histamine-IAI Trisaccharide Complexes[a,b,c]

	monosaccharide conformations			IA linkage	AI linkage	energy of the complex kcal/mol			average distance from imidazole to: (Å)	
complex	I′	A	I″	Φ,Ψ	Φ,Ψ	intermolecular	intramolecular	total	A-H3	A-H5
1/N	$^1C_4$	$^4C_1$	$^1C_4$	45, −11	−59, −40	−65.4	30.7	−34.7	2.6	4.7
1/O	$^1C_4$	$^4C_1$	$^1C_4$	46, 9.0	−41, −21	−58.8	26.9	−31.9	3.3	5.8
2/N	$^1C_4$	$^4C_1$	$^1C_4$	−40, −30	−40, −20	−62.6	31.3	−31.3	2.9	3.8
2/O	$^1C_4$	$^4C_1$	$^1C_4$	−40, −48	−40, −20	−64.6	33.9	−30.7	3.1	5.9
3/N	$^2S_0$	$^4C_1$	$^2S_0$	66, −10	−50, −60	−48.9	33.1	−15.8	3.4	3.0
3/O	$^2S_0$	$^4C_1$	$^2S_0$	86, −10	−30, −60	−59.3	35.6	−23.7	2.8	4.7

[a] IAI represents the oligosaccharide IdoA(2S)-(1→4)-GlcNS(6S)-(1→4)-IdoA(2S). [b] In complexes 1 and 3, the two carboxylate groups are on the opposite sides of the IAI oligosaccharide; in 2 they are on the same side. [c] The N and O labels refer to different orientations of histamine in the binding cleft, as discussed in the text.

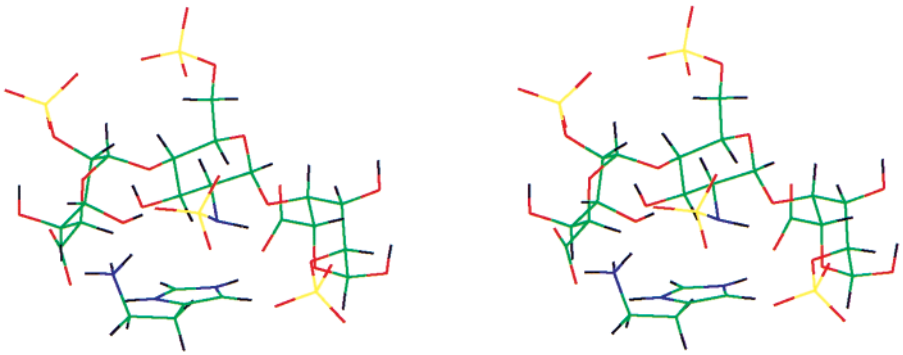

FIGURE 10: Stereoview of a stick model of complex 1/N. The complex is oriented with the reducing end of the IAI trisaccharide on the right (I′AI″) and the ammonium tail of histamine facing out of the plane of the paper (the N orientation).

complexes and justifying the 2.5−3.5 Å distance constraint assigned in the grid search. Quantitative ring current shifts associated with imidazole have not been predicted, however, the 0.50 ppm upfield shift observed for Ad-H3 of **III** is reasonable at distances in the 2.5−3.5 Å range, based on ring current shifts predicted for benzene (*50*). At 3 Å above its center, benzene would induce a 2 ppm upfield shift; however the corresponding effect for imidazole is expected to be smaller (*57*). Moreover, since each histamine binding site is occupied for only a fraction of the time, the observed A−H3 chemical shifts are a time average of the chemical shifts of the bound and unbound states. Consequently, the observed upfield shifts in Ab-H3 and Ad-H3 would tend toward the lower value, as was observed.

Manual docking also revealed that histamine fit into the binding cleft equally well in two distinct (N and O) orientations. In the structure in Figure 10, the IAI trisaccharide is oriented with its nonreducing end on the left. Histamine is docked to the trisaccharide in the N orientation, i.e., with its ammonium group projecting out of the plane of the paper and adjacent to the N-sulfate of the A ring. In the O orientation (not shown), histamine is rotated 180° with the ammonium tail projecting into the plane of the paper so that it lies on the opposite side of the heparin chain (the heparin surface containing the 6-O-sulfate group of the A ring). A significant energy barrier was found to separate the N and O orientations so that if the grid search was initiated with histamine in one of these orientations, the other orientation would not be sampled. Independent grid searches with histamine in the N and O orientations were performed in order to sample both of these regions of the conformational space of the complex. Ultimately, a total of six grid searches was completed on the three unique IAI trisaccharides with histamine positioned in the N and O orientations.

The structural parameters and energies of the complexes obtained from the grid search calculations are summarized in Table 5. The values reported in Table 5 correspond to those of the lowest energy complex identified in each grid search. The total energy of each complex is a sum of intramolecular and intermolecular components. The positive intramolecular energies are a result of bonded strain energy and positive Coulombic energy associated with the repulsion of "like" formal charges within each molecule independent of the other. The large and negative intermolecular energies are entirely nonbonded and are due primarily to the strong Coulombic interactions between the positively charged histamine and the negatively charged trisaccharide.

Complex 1/N (Figure 10) was found to be the most stable with an energy of −34.7 kcal/mol. The relatively low intramolecular term (30.7 kcal/mol) was traced to a low strain energy in the ϕ_{IA} torsion angle at 45°, which results from the stabilizing action of the exoanomeric effect at ϕ angles near +60° for an L sugar.[4] The intermolecular energy is more attractive than for any other complex as a result of favorable

[4] The exoanomeric effect had been explicity incorporated into the Amber force field by Homans (*39*) for D sugars using the following parameters for the ϕ torsional potential: for OE-AC-OA-CS, $V_1 = 2.15$ and $\phi_1 = 300°$; for AH-AC-OA-CS, $V_2 = 1.75$ and $\phi_2 = 60°$; and for CS-AC-OA-CS, $V_3 = 0.85$ and $\phi_3 = 0°$ where OE, AC, etc., are atom types as defined by Homans and the units for V_1, V_2 and V_3 are kcal/mole. These parameters were modified so that mirror image structures of methyl D-iduronic acid and methyl L-iduronic acid yielded equivalent energies at all ϕ angles. To incorporate this modification, LC, OL, and LH were added as new atom types that represent the α-L sugar anomeric carbon, anomeric oxygen, and anomeric hydrogen, respectively. The corresponding parameters for the L sugar are: for OE-LC-OL-CS, $V_1 = 2.15$ and $\phi_1 = 60°$; for LH-LC-OL-CS, $V_2 = 1.75$ and $\phi_2 = 300°$; and for CS-LC-OL-CS, $V_3 = 0.85$ and $\phi_3 = 0°$. All other parameters, except the three listed above, were equivalent to Homans' parameters for an α-D sugar.

Table 6: Charge Pairs with a Separation Less than 3 Å in the Histamine−IAI Trisaccharide Complexes[a,b]

complex	charge pairs			
1/N	Im(N1H)-I′(CO_2)	Im(N3H)-I″(CO_2)	His(NH_3)-A(NSO_3)	
1/O	Im(N3H)-I′(CO_2)	Im(N1H)-I″($2SO_4$)	His(NH_3)-I″(CO_2)	
2/N	Im(N1H)-I′(CO_2)	Im(N3H)-I″(CO_2)	His(NH_3)-I″($2SO_4$)	
2/O	Im(N1H)-I″($2SO_4$)	Im(N3H)-I″($2SO_4$)	His(NH_3)-I″(CO_2)	His(NH_3)-I′(CO_2)
3/N	Im(N1H)-I′($2SO_4$)	Im(N3H)-I″(CO_2)		
3/O	Im(N1H)-I″(CO_2)	His(NH_3)-A($6SO_4$)		

[a] The monosaccharide conformations of the trisaccharides and the ϕ, ψ angles are given in Table 5. [b] The <3 Å distance refers to the distance between the NH proton and the nearest oxygen of the anionic site.

pairing of negative charges on heparin with positive charges on histamine. The structure in Figure 10 shows the 1/N complex with the imidazolium ring in the binding cleft formed by the A ring and the two I rings. The imidazolium N1H proton is directly paired with the I′ carboxylate and the imidazolium N3H proton is paired with the I″ carboxylate.[1] The distance from each imidazolium NH proton to the nearest oxygen of its carboxylate partner is approximately 1.8 Å. I′ and I″ carboxylates are positioned on opposite sides of the heparin chain. Other significant pairing involves the ammonium group of histamine and the N-sulfate group of the A residue, with a distance of 2 Å between an NH_3 proton and an N-sulfate oxygen. All other sulfates are farther than 5 Å from the histamine imidazolium and ammonium NH protons. On average, the imidazole ring protons are 2.6 Å from the A3 proton. This separation is less than that exhibited by the other complexes, suggesting that this complex yields the best steric fit for the docking of the two molecules. Complex 1/O is 2.8 kcal/mol higher in energy than 1/N even though the heparin structures and binding site in both complexes are nearly equivalent.

The $(\phi/\psi)_{IA}$ angles of 2/N and 2/O (Table 5) are quite distinct from those of 1/N and 1/O and are for heparin structures with the I′ and I″ carboxylates positioned on the same side of the chain, i.e., the side of the chain containing the 6-O-sulfate. The 2/N and 2/O complexes exhibited a different pairing of charge groups (Table 6) that was somewhat less favorable than the pairing in 1/N, but the primary source of their higher total energy is the increased torsional strain associated with the $-40°$ ϕ_{IA} torsional angle.

The third set of complexes, 3/N and 3/O, was constructed with I′ and I″ fixed in the $^2S_0$ conformation. These complexes were studied to assess whether the $^2S_0$ conformation would result in complexes as stable as the complexes constructed with the I rings in the $^1C_4$ conformation. The heparin chain in the 3/N and 3/O complexes was more extended and the well-defined pocket formed by the IAI triad in complexes 1 and 2 was absent. The mutual pairing of histamine and heparin charge groups was minimized (Table 6) with the loss of this pocket. For example, in complex 3/O, the imidazole N1H proton interacts with the I″ CO_2^- group, but the imidazole N3H proton is over 3.5 Å in distance from any heparin sulfate or carboxylate oxygen.

DISCUSSION

Previous ^{1}H NMR studies of the binding of histamine by heparin have established that heparin binds histamine site-specifically in a complex, which positions the A−H3 proton within the shielding cone of the imidazolium ring and that the binding is mediated primarily by electrostatic interactions (*6*, *7*). The goal of the present study was to determine the minimum requirements of the binding site for site-specific binding and to identify specific interactions involved in the binding.

Focusing first on histamine, the binding of imidazole by hexasaccharide **III** was studied to determine if the ammonium group of histamine is essential for site-specific binding. The results indicate that the imidazolium ion by itself binds site-specifically to sites Ab and Ad of **III**. However, the $\Delta\delta$ values for both Ab-H3 and Ad-H3 are smaller in the presence of imidazole, which indicates that, while the imidazolium group of histamine is critical in directing site-specific binding, the ammonium group enhances the binding interaction.

The results for the binding of histamine by the heparin-derived oligosaccharides and chemically modified heparins in Figure 1 establish that the IAI triad is the minimum heparin sequence, which binds histamine site-specifically. The ring current shift induced by the imidazolium ring in the A−H3 resonance locates the histamine adjacent to the A ring. The absence of site-specific binding to Ab of disaccharide **I**, Ad of tetrasaccharide **II** and Af of hexasaccharide **III** indicates that a uronic acid is required at the reducing end of the A ring for site-specific binding, while the relative magnitudes of the $\Delta\delta$s for Ab-H3 and Ad-H3 of **III** establish the importance of the I-ring at the nonreducing end of the IAI sequence. The results obtained with pentasaccharide **VI** and chemically modified heparin **VIII** establish that the 2-O-sulfate groups on the I rings are not essential for binding. Similarly, the results obtained with hexasaccharide **V** and chemically modified heparin **X** establish that the 6-O-sulfate group on the A ring is not essential for site-specific binding. These results are consistent with the minimum-energy structure (1/N) obtained from the molecular modeling calculations (Figure 10 and Table 6). The absence of site-specific binding to chemically modified heparins **IX** and **XI** provides strong evidence that the sulfamido group of the A-ring is essential for site specific binding, which also is consistent with the minimum energy structure (1/N) from the molecular modeling calculations. The ring-current-induced upfield shifts of the resonances for Ab-H3 and Ad-H3 (Figure 8) over the pD range where the carboxylic acid groups of ΔUa, Ic, and Ie of hexasaccharide **III** are titrated (Figure 6) indicates that the carboxylic acid groups, in their deprotonated carboxylate form, are essential for site specific binding.

The absence of site-specific binding at residue Ad of hexasaccharide **IV** establishes that the configuration of the carboxylate group of the uronic acid residue linked to the reducing end of the A ring is critical for binding. Also, the

results in Table 4 indicate that histamine binds to the IAI triad with the I rings in the $^1C_4$ conformation. This is confirmed by the results in Table 5 where the energies calculated for the complexes with the I rings in the $^2S_0$ conformations are substantially higher. These results further highlight the site-specific nature of the binding.

The chemical shift vs pD titration curve for Ie-H5 of hexasaccharide **III** in the presence of histamine (Figure 7) shows a somewhat different behavior than that observed for ΔUa-H4 and Ic-H5. As the pD is increased, the chemical shift of Ie-H5 parallels that of free **III** up to pD ∼ 5, it then remains approximately constant up to pD ∼ 7, and then shifts back to that of free **III** as the pD is increased further. This different behavior reflects not only the deprotonation of the Ie carboxylic acid group but also the change in the position of the $^1C_4 \rightleftharpoons {}^2S_0$ conformational equilibrium. Specifically, as the pD is increased from ∼2, site-specific binding of histamine at site Ad causes titration of the Ie carboxylic acid group at a lower pD, which causes the upfield titration shift of the resonance for Ie-H5 to be displaced to lower pD. However, at the same time, binding of histamine causes the conformational equilibrium of Ie to shift, which causes the chemical shift of the exchange-averaged resonance for Ic-H5 to shift toward that of the $^1C_4$ conformation. Chemical shift data for Ic-H5 and Ie-H5 of **III** indicate that the chemical shift of the I−H5 resonance for the $^1C_4$ conformation is downfield from that for the $^2S_0$ conformation. Specifically, in the absence of histamine, the Ic and Ie residues are 60 and 45% in the $^1C_4$ conformations, respectively, while the chemical shifts of the resonances for Ic-H5 and Ie-H5 at pD ∼ 6 are 4.852 and 4.789 ppm.

The molecular modeling results provide additional insight into the nature of the site-specific binding. In the molecular modeling study, the energy was minimized for the binding of histamine by the three conformations of the IAI trisaccharide in Table 5, using as the only constraint that the A−H3 proton be positioned above and in the shielding cone of the imidazolium ring. Complex 1/N in Table 5 proved to be the most energetically stable and its structure is consistent with the experimental data. A steroview of a stick model of complex 1/N is shown in Figure 10. A well-defined pocket is formed in which histamine can dock, while maintaining the required orientation of the imidazolium ring relative to the A−H3 proton. The imidazolium ring nuclei are located only 2.8 Å from A−H3 with introduction of little steric strain in the heparin trisaccharide suggesting a good steric fit of histamine in the pocket. Carboxylates assume an essential role in charge-pairing with the histamine. The imidazolium N1H proton is hydrogen bonded to the carboxylate of the I′ ring while the imidazolium N3H proton is hydrogen bonded to the carboxylate of the I″ ring (Figure 10 and Table 6). This bidentate interaction of heparin with the imidazolium ring was found to be the most favorable and is consistent with the experimental data. The requirement for the I″ carboxylate was clearly demonstrated by the experimental results for the binding of histamine to oligosaccharides **I**, **II**, and **III**, and the influence of the I′ carboxylate has been inferred from the relative magnitudes of the Δδs for Ab-H3 and Ad-H3 of hexasaccharide **III**. The structure of 1/N demonstrates the viability of a complex in which the carboxylates of both I residues of the IAI triad can intimately interact with site-specifically bound histamine.

The results in Table 6 indicate that the complex is stablized by interaction of the ammonium group of histamine with the N-sulfate group of the A ring. This is consistent with more binding of histamine than imidazolium ion by **III**, as indicated by the relative magnitudes of the $\Delta\delta$ values for Ab-H3 and Ad-H3.

The conformational flexibility of the iduronate residue contributes to the versatility and specificity of the interaction of heparin with biological molecules (*41*, *50*−*53*, *58*). For example, in recently reported X-ray structures of basic fibroblast growth factor with bound tetrasaccharide **II** and hexasaccharide **III**, the IdoA(2S) residue at position c of bound **II** was found to be in the $^1C_4$ conformation, while those at positions c and e of **III** were found to be in the $^1C_4$ and $^2S_0$ conformations, respectively (*41*). In contrast, residue c of **II** free in solution and residues c and e of **III** free in solution exist as an equilibrium mixture of the $^2S_0$ and $^1C_4$ conformations (*58*, *59*). A comparison of the total energies of the six complexes in Table 5 indicates that the $^1C_4$ conformation provides the more energetically favored histamine binding pocket. The oligosaccharide chain in the 3/N and 3/O complexes is more extended and the well-defined cleft formed by the IAI trisaccharide in complexes 1 and 2 is absent. Furthermore, extension of the oligosaccharide chain reduced the charge pairing interactions (Table 6). The less favorable binding identified in the 3/N and 3/O complexes with the $^2S_0$ conformation is consistent with the experimentally observed shift in the conformational equilibrium of the I ring to the $^1C_4$ conformation upon binding of histamine by **III**.

CONCLUSIONS

The experimental and theoretical results reported here provide a detailed picture of the site-specific binding of histamine by heparin. The results indicate that the most important feature of the site-specific binding is the location of the imidazolium group in a cleft formed by the IAI triad with the two imidazolium NH protons hydrogen bonded to the carboxylate groups of the two I residues, while the additional interaction of the ammonium group with the N-sulfate group of the A residue enhances the binding interaction. Given the similarity of the NMR results for the binding of histamine, *N*-acetylhistamine, and the tripeptide glycyl-histidyl-lysine by heparin, we propose that the imidazolium groups of the histidine side chains of β-amyloid peptide (*21*) and mouse mast cell protease 7 (*22*) bind to heparin in the same binding cleft.

REFERENCES

1. Lagunoff, D. (1975) in *Techniques of Biochemical and Biophysical Morphology* (Glick, D., and Rosenbaum, R., Eds.) pp 283−305, John Wiley, New York.
2. Kruger, P. G., and Lagunoff, D. (1981) *Int. Arch. Allergy Apply. Immunol. 65*, 291−299.
3. Rabenstein, D. L., Ludowyke, R., and Lagunoff, D. (1987) *Biochemistry 26*, 6923−6926.
4. Martin, T. W., and Lagunoff, D. (1984) in *Mast Cell Secretion* (Cantin, M., Ed.) pp 481−516, S. Karger, Basel.
5. Lagunoff, D. (1974) *Biochemistry 13*, 3982−3986.
6. Rabenstein, D. L., Bratt, P., Schierling, T. D., Robert, J. M., and Guo, W. (1992) *J. Am. Chem. Soc. 114*, 3278−3285.
7. Rabenstein, D. L., Bratt, P., and Peng, J. (1998) *Biochemistry 37*, 14121−14127.

8. Casu, B. (1989) in *Heparin: Chemical and Biological Properties, Clinical Applications* (Lane, D. A., and Lindahl, U., Eds.) pp 25−49, CRC Press, Boca Raton, FL.
9. Gatti, G., Casu, B., Hamer, G. K., and Perlin, A. S. (1979) *Macromolecules 12*, 1001−1007.
10. Diakun, G. P., Edwards, H. E., Wedlock, D. J., Allen, J. C., and Phillips, G. O. (1978) *Macromolecules 11*, 1110−1114.
11. Mattai, J. and Kwak, J. C. T. (1981) *Biochim. Biophys. Acta 677*, 303−312.
12. Olson, S. T., Halvorson, H. R., and Bjork, I. (1991) *J. Biol. Chem. 266*, 6342−6352.
13. Olson, S. T., and Bjork, I. (1991) *J. Biol. Chem. 266*, 6353−6364.
14. Mascotti, D. P., and Lohman, T. M. (1995) *Biochemistry 34*, 2908−2915.
15. Rabenstein, D. L., and Robert, J. M., and Peng, J. *Carbohydr. Res. 278*, 239−256.
16. Manning, G. S. (1979) *Acc. Chem. Res. 12*, 443−449.
17. Manning, G. S. (1978) *Q. Rev. Biophys. 11*, 179−246.
18. Johnson, R. G., Carty, S. E., Fingerhood, B. J., and Scarpa, A. (1980) *FEBS Lett. 120*, 75−79.
19. Lagunoff, D., and Rickard, A. (1983) *Exp. Cell Res. 144*, 353−360.
20. D. L. Rabenstein, J. M. Robert, and Hari, S. (1995) *FEBS Lett. 376*, 216−220.
21. Brunden, K. R., Richter-Cook, N. J., Chaturvedi, N., and Frederickson, R. C. A. (1993) *J. Neurochem. 61*, 2147−2154.
22. Matsumoto, R., Sali, A., Ghildyal, N., Karplus, M., and Stevens, R. L. (1995) *J. Biol. Chem. 270*, 19524−19531.
23. Snow, A. D., Mar, H., Nochlin, D., Kimatoa, K., Sato, M., Suzuki, S., Hassell, J., and Wight, T. N. (1988) *Am. J. Pathol. 133*, 456−463.
24. Linhardt, R. J. and Toida, T. (1997) in *Carbohydrates in Drug Design* (Witczak, Z. J., and Nieforth, K. A., Eds.) pp 277−341, Marcel Dekker, Inc, New York.
25. Rice, K. G., and Linhardt, R. J. (1989) *Carbohydr. Res. 190*, 219−233.
26. Sugahara, K., Tsuda, H., Yoshid, K., Yamada, S., Beer, T. de., and Vliegenthart, F. G. (1995) *J. Biol. Chem. 270*, 22914−22923.
27. Jaseja, M., Rej, R. N., Sauriol, F., and Perlin, A. A. (1989) *Can. J. Chem. 67*, 1449−1456.
28. Nagasawa, K., and Inoue, Y. (1980) *Methods Carbohyd. Chem. 8*, 287−289.
29. Yates, E. A., Santini, F., Guerrini, M., Naggi, A., Torri, G., and Casu, B. (1996) *Carbohydr. Res. 294*, 15−27.
30. Bax, A., and Davis, D. G. (1985) *J. Magn. Reson. 65*, 355−360.
31. Davis, D. G., and Bax, A. (1985) *J. Am. Chem. Soc. 107*, 2820−2821.
32. Bothner-By, A. A., Stephens, R. L., Lee, J.-M., Warren, C. D., and Jeanloz, R. W. (1984) *J. Am. Chem. Soc. 106*, 811−813.
33. Bax, A., and Davis, D. G. (1985) *J. Magn. Reson. 63*, 207−213.
34. States, D. J., Habercorn, R. A., and Ruben, D. J. (1982) *J. Magn. Reson. 48*, 286−292.
35. Bax, A., and Davis, D. A. (1985) *J. Am. Chem. Soc. 107*, 7197−7199.
36. Rance, M. (1987) *J. Magn. Reson. 74*, 557−564.
37. Castellano, S., and Bothner-By, A. A. (1964) *J. Chem. Phys. 41*, 3863−3869.
38. Ferro, D. R., Provasoli, A., Ragazzi, M., Torri, G., Casu, B., Gatti, G., Jacquinet, J.-C., Sinay, P., Petitou, M., and Choay, J. (1986) *J. Am. Chem. Soc. 108*, 6773−6778.
39. Homans, S. W. (1990) *Biochemistry 29*, 9110−9118.
40. Huige, C. J. M., and Altona, C. (1995) *J. Comput. Chem. 16*, 56−79.
41. Faham, S., Hileman, R. E., Fromm, J. R., Linhardt, R. J., and Rees, D. C. (1996) *Science 271*, 1116−1120.
42. Chamberlin, L. N., Edwards, I. A. S., Stadler, H. P., Buchanan, J. G., and Thomas, A. W. (1981) *Carbohydr. Res. 90*, 131−137.
43. Yamada, S., Yamane, Y., Tsuda, H., Yoshida, K., and Sugahara, K. (1998) *J. Biol. Chem. 273*, 1863−1871.
44. Chai, W., Hounsell, E. F., Bauer, C. J., and Lawson, A. M. (1995) *Carbohydr. Res. 269*, 139−156.
45. Pervin, A., Gallo, C., Jandik, K. A., Han, X.-J., and Linhardt, R. J. (1995) *Glycobiology 5*, 83−95.
46. Larnkjaer, A., Hansen, S. H., and Ostergarrd, P. B. (1995) *Carbohydr. Res. 266*, 37−52.
47. Hileman, R. E., Smith, A. E., Toida, T., and Linhardt, R. J. (1997) *Glycobiology 7*, 231−239.
48. Sanderson, P. N., Hucherby, T. N., and Nieduszynski, I. A. (1987) *Biochem J. 243*, 175−181.
49. Ernst, S., Venbkataraman, G., Sasisekharan, V., Langer, R., Cooney, C. L., and Sasisekharan, R. (1998) *J. Am. Chem. Soc. 120*, 2099−2107.
50. van Boeckel, C. A. A., van Aelst, S. F., Wagenaars, G. N., Mellema, J.-R., Pausenn, H., Peters, T., Pollex, A., and Sinnwell, V. (1987) *Recl. Trav. Chim. Pays-Bas 106*, 19−29.
51. Ferro, D. R., Provasoli, A., Ragazzi, M., Casu, B., Torri, G., Bossennec, V., Perly, B., Sinay, P., Petitou, M., and Choay, J. (1990) *Carbohyd. Res. 195*, 157−167.
52. Cros, S., Petitou, M., Sizun, P., Perez, S., and Imberty, A. (1997) *Bioorg. Medic. Chem. 5*, 1301−1309.
53. Mulloy, B., Forster, M. J., Jones, C., and Davies, D. B. (1993) *Biochem. J. 293*, 849−858.
54. Ragazzi, M., Ferro, D. R., Provasoli, A., Pumilia, P., Cassinari, A., Torri, G., Guerrini, M., Casu, B., Nader, H. B., and Dietrich, C. P. (1993) *J. Carbohydrate Chem. 12*, 523−535.
55. Bazin, H. G., Capila, I., and Linhardt, R. J. (1998) *Carbohydr. Res. 309*, 135−144.
56. Bovey, F. A. (1988) *Nuclear Magnetic Resonance Spectroscopy*, Academic Press, New York.
57. Perkins, S. J. (1982) in *Biological Magnetic Resonance* (Berliner, L. J., and Reuben, J. Eds.) Vol. 4, pp 193−336, Plenum Press, New York.
58. Mikhailov, D., Linhardt, R. J., and Mayo, K. H. (1997) *Biochem. J. 328*, 51−61.
59. Mikhailov, D., Mayo, K. H., Vlahov, I. R., Toida, T., Pervin, A., and Linhardt, R. J. (1996) *Biochem. J. 318*, 93−102.

BI9926025